**Cite this article**
Klinkvort RT, Bienen B, Fan S *et al.* (2026)
Centrifuge modelling considerations of laterally loaded monopiles in sand.
*International Journal of Physical Modelling in Geotechnics* **26(2)**: 93–104,
https://doi.org/10.1680/jphmg.25.00046

**Research Article**
**Paper 2500046**
Received 05/08/2025; Accepted 15/10/2025



**International Journal of Physical Modelling in Geotechnics**

# Centrifuge modelling considerations of laterally loaded monopiles in sand

**Rasmus Tofte Klinkvort**
Norwegian Geotechnical Institute, Oslo, Norway (corresponding author: rtk@ngi.no)

**Britta Bienen**
Centre for Offshore Foundation Systems, School of Earth and Oceans, University of Western Australia, Perth, Australia

**Shengsheng Fan**
Fugro Australia Pty Ltd, Perth, Australia; Centre for Offshore Foundation Systems, School of Earth and Oceans, University of Western Australia, Perth, Australia

**Jonathan Black**
School of Natural and Built Environment, Queen's University Belfast, Belfast, Northern Ireland; Department of Civil & Structural Engineering, Centre for Energy and Infrastructure Ground Research, University of Sheffield, Sheffield, England

**Steven Bayton**
Multiconsult, Oslo, Norway; Norwegian Geotechnical Institute, Oslo, Norway; Department of Civil & Structural Engineering, Centre for Energy and Infrastructure Ground Research, University of Sheffield, Sheffield, England

**Luc Thorel**
Centrifuges for Geotechnics Laboratory, Université Gustave Eiffel, Nantes, France

**Matthieu Blanc**
Centrifuges for Geotechnics Laboratory, Université Gustave Eiffel, Nantes, France

**Gopal Santana Phani Madabhushi**
Department of Engineering, University of Cambridge, Cambridge, England

**Stuart K. Haigh**
Department of Engineering, University of Cambridge, Cambridge, England

**Thomas Broad**
Department of Engineering, University of Cambridge, Cambridge, England

**Varvara Zania**
Department of Environmental and Resource Engineering, Technical University of Denmark, Lyngby, Denmark

**Amin Askarinejad**
Department of Geoscience and Engineering, Delft University of Technology, Delft, The Netherlands

**Qiang Li**
Powerchina Huadong Engineering Corporation Limited, Shenzhen, China; Department of Geoscience and Engineering, Delft University of Technology, Delft, The Netherlands

**Dong Soo Kim**
Department of Civil and Environmental Engineering, Korea Advanced Institute of Science and Technology, Daejeon, South Korea

**Sunji Park**
Department of Civil and Environmental Engineering, Korea Advanced Institute of Science and Technology, Daejeon, South Korea

**Luke J. Prendergast**
Department of Civil Engineering, Faculty of Engineering, University of Nottingham, Nottingham, England

**Kunkun Cheng**
Department of Civil Engineering, Faculty of Engineering, University of Nottingham, Nottingham, England

**Charles Heron**
Department of Civil Engineering, Faculty of Engineering, University of Nottingham, Nottingham, England

**Alec Marshall**
Department of Civil Engineering, Faculty of Engineering, University of Nottingham, Nottingham, England

**Marcio De Souza Soares de Almeida**
Graduate School of Engineering, COPPE/UFRJ, Federal University of Rio de Janeiro, Rio de Janeiro, Brazil

**Maria Fernanda Barra**
Graduate School of Engineering, COPPE/UFRJ, Federal University of Rio de Janeiro, Rio de Janeiro, Brazil

**The large-diameter monopile is a commonly used foundation concept for offshore wind turbines. The advantages of geometrical simplicity and reliable performance make it often the most attractive solution. Despite the concept's high popularity, optimisation of the current design models can still be made. To address fundamental understanding of modelling effects in centrifuge testing of laterally loaded monopiles in sand, a large coordinated centrifuge-testing programme across nine different centrifuge centres worldwide has been conducted. This paper presents firstly the results of a local benchmark modelling of model test series performed in two centrifuges and secondly the results of global benchmark testing across the nine centrifuges. The results highlight the reliability of centrifuge testing as it was possible to model a similar prototype response in both the local and global benchmark tests, despite differences in the experimental setups and pile geometries. Furthermore, as examples of the modelling technique, two different cases are presented, one showing the effect of installation and one showing the effect of pile penetration depth. Finally, recommendations are provided to enhance centrifuge testing of monopile response under complex loading.**

**Keywords:** centrifuge modelling/monopile/sands

## Notation

| | |
|---|---|
| $D$ | pile diameter |
| $D_{CPT}$ | diameter of penetrometer |
| $D_{proto}$ | prototype pile diameter |
| $D_r$ | relative density |
| $d_{50}$ | average sand grain size |

| | |
|---|---|
| $E_p$ | pile stiffness |
| $g$ | gravity |
| $G_0$ | initial shear stiffness |
| $H$ | applied horizontal load |
| $I_p$ | pile area moment of inertia |
| $k$ | permeability |
| $l_e$ | load eccentricity |
| $l_L$ | pile penetration length |
| $l_t$ | thickness of pile |
| $M$ | modulus stiffness |
| $N$ | scaling factor |
| $r_0$ | rotation at soil surface |
| $R_a$ | roughness factor |
| $R_{\mathrm{eq}}$ | equivalent radius |
| $R_t$ | radius from centre of rotation to soil surface |
| $t$ | time |
| $V$ | applied vertical load |
| $Y$ | pile head displacement |
| $y_0$ | pile displacement at soil surface |
| $y_1$ | pile displacement at height 1 |
| $y_2$ | pile displacement at height 2 |
| $y_{top}$ | pile displacement at the top of the pile |
| $z$ | depth below soil surface |
| $z_1$ | height 1 |
| $z_2$ | height 2 |
| $\gamma$' | effective unit weight |
| $\varphi$' | effective angle of friction |
| $\omega$ | rotational frequency |

## 1. Introduction

Monopile foundations are still the preferred foundation solution for offshore wind turbines, due to the simple geometry (a hollow steel pile) and the experience gathered over the years (Wind Europe, 2018). However, despite their wide use and continuous optimisation, there are still areas of uncertainty in monopile design. From a geotechnical perspective, these uncertainties relate to the interaction between soil, structure, and loads. Offshore wind turbines are dynamically sensitive structures that are subjected to complex loading from the wind, the waves, and the current. These loads are always cyclic and often also multidirectional. One of the key factors of the dynamic response of the wind turbine is the stiffness of the monopile.

Significant research attention has been directed to the lateral response of monopiles. The majority of the research focused on the cyclic response, as this reflects the nature of the offshore environmental loading condition. For example, Cuéllar *et al*. (2009), LeBlanc *et al*. (2010) and Peralta and Achmus (2010), Li *et al*. (2010), Klinkvort (2012), Rudolph *et al*. (2014), Kirkwood (2015), Truong and Lehane (2015), Bayton and Black (2016) and Choo and Kim (2016), Truong *et al*. (2019), Bienen *et al*. (2021), and Takahashi *et al*. (2022).

In most of the published model testing, the monopiles were installed by jacking at 1 g. Fan *et al*. (2019) compared the lateral monopile response after impact or jacking installation in loose sand. Although it is known that the state of the surrounding soil and the subsequent lateral response are significantly influenced by the pile installation method, little has been published in this respect. Some numerical work, for example, presented in Bienen *et al*. (2021) or Staubach *et al*., 2022 have confirmed the few observations seen in the centrifuge. On the other hand, for the case of pile axial behaviour, it is widely documented that the response is strongly influenced by the installation method, as indicated by De Nicola and Randolph (1997), Mahutka *et al*. (2006), Henke and Grabe (2008), and Henke and Bienen (2014). Where piles have been jacked or impact driven in-flight in centrifuge tests (Dyson and Randolph, 2001; Klinkvort, 2012), the requirement for stopping of the centrifuge was necessary to mount the lateral loading rig; a procedure with unquantified and questionable effects on the lateral response. The experimental series performed by Truong *et al*. (2019) was carried out after a jacked in-flight installation at the same g field; however, a comparison with 1 g pile installation was not presented. Hence, the effect of the pile installation process on the lateral response still remains uncertain.

Besides the aforementioned, the continued lack of a fundamental understanding of monopile behaviour has also been highlighted by a review of the effects influencing the response of a monopile in the centrifuge (Klinkvort *et al*., 2018). Based on this review and inspired by the multi-facility research on cone penetration test (CPTs) presented in Bolton *et al*. (1999), this paper presents results from a multi-facility test programme that investigated fundamental centrifuge modelling considerations underpinning the testing of monopiles in a centrifuge. The primary purpose of the paper is to demonstrate that, through careful design and normalisation of test results, similar results can be obtained in different centrifuge setups with various geometries and loading setups. This validates the centrifuge modelling theory and provides credibility to centrifuge testing of monopiles in sand in general. Secondly, we show some simple examples of how centrifuge modelling can be used to explore different mechanisms.

The test programme was conducted at different centrifuges with different setups, sizes, model monopiles, and sands. Through careful design of the testing programme, several of the effects that control the lateral response of a monopile were investigated. The study focuses on the monotonic lateral response of the monopile, but many of the findings are also valid for more complex load situations.

## 2. Experimental methodology

The multi-facility monopile testing was carried out in nine different centrifuge facilities and soil testing at the Norwegian Geotechnical Institute (NGI). The centrifuge facilities in question are located at the Centre for Engineering Infrastructure Ground Research (CEIGR) at the University of Sheffield, the Centre for

Offshore Foundation Systems at the University of Western Australia (COFS), The Alberto Luiz Coimbra Institute for Graduate Studies and Research in Engineering at The Federal University of Rio de Janeiro (COPPE), University of Cambridge Engineering Department (CUED), Technical University of Denmark (DTU), University Gustave Eiffel (UGE), Korea Advanced Institute of Science & Technology (KAIST), Technical University of Delft (TU Delft), and University of Nottingham (UoN).

All testing was performed in beam centrifuges. Figure 1 shows a schematic of a beam centrifuge, where the model is placed on a swing basket located at the end of a rotating arm. The nine centrifuges have different sizes, actuators, and data acquisition techniques, but the testing principles are the same for all of them. Soil response is stress dependent, and the increased acceleration in the centrifuge allows to test models in stress conditions similar to the prototype. The principles and physics governing stress similitude are well defined after the extensive centrifuge testing of geotechnical applications in the past decades (Taylor, 1994).

The increase in vertical stress as a function of depth is not linear in the centrifuge because of the increase of the radius, and a complete stress similitude throughout the depth of the model is therefore not possible. For pile testing, the stress error is minimised by securing exact stress similitude at 2/3 of the pile penetration. The scaling factor for the testing can then be found using an equivalent radius $R_{eq} = R_t + l_L/3$, that is found as half the depth of the reference point and the radius to the sand surface, see Taylor (1994) for greater details.

1. $$N = \frac{R_{eq}\omega^2}{g}$$

where, $\omega$ = rotational frequency and $g$ = gravity. Having achieved stress similitude, this allows the measurements obtained in the centrifuge to be related to prototype behaviour by a geometrical linear normalisation through dimensional analysis (Garnier *et al.*, 2007 provides a general overview of scaling relations). For the lateral response of a monopile in sand, this leads to a function for the lateral response that is described by a series of normalised parameters (Equation 2):

2. $$\frac{H}{\gamma' D^3} = f\left(\frac{Y}{D}, \frac{l_L}{D}, \frac{l_e}{D}, \frac{I_p}{D^4}, \frac{E_p}{\gamma' D}, \frac{G_0}{\gamma' D}, \frac{Mkt}{\gamma_w D^2}, \varphi', \frac{l_t}{d_{50}}, \frac{D}{d_{50}}, \frac{R_a}{d_{50}}\right)$$

where $H$ = applied horizontal load; $Y$ = pile head displacement; $D$ = pile diameter; $\gamma'$ = effective unit weight; $l_L$ = pile length; $l_e$ = load eccentricity; $I_p$ = pile area moment of inertia; $E_p$ = pile stiffness; $G_0$ = Initial shear stiffness, $M$ = modulus stiffness; $k$ = permeability; $t$ = time; $\gamma_w$ = effective unit weight of water; $\phi'$ = effective angle of friction; $l_t$ = thickness of the pile wall; $d_{50}$ = average sand grain size; and $R_a$ = roughness factor.

Full similitude between the centrifuge model and the prototype may not always be possible to achieve in all aspects, and this paper investigates the effects of this.

To allow comparison, including comparison beyond this benchmarking exercise, it is necessary to relate the pile response to a common reference point, which is chosen here at the sand surface. Because it is not possible to have any measurement transducers at this point, displacements need to be transferred to this reference point, as indicated schematically in Figure 2. The displacement of the pile above the soil surface can be described by Equation 3 using Euler–Bernoulli beam theory.

3. $$y(z) = y_0 - z \cdot r_0 + \frac{Hz^2}{6E_pI_p}(3l_e + z)$$

Where $y_0$ = displacement at soil surface, $r_0$ = rotation at soil surface, and $z$ = depth below surface.

The displacements ($y_1$ and $y_2$) are measured at two different heights ($z_1$ and $z_2$) during the experiments, and the rotation at the soil surface can be found as follows:

4. $$r_0 = \frac{y_1 - y_2 + \frac{H}{6EI}\left(z_2{}^2(3l_e - z_2) - z_1{}^2(3l_e - z_1)\right)}{(z_1 - z_2)}$$

The displacement at the soil surface can then be found as shown in Equation 5.

5. $$y_0 = y_1 - z_1 \cdot r_0 - \frac{Hz_1{}^2}{6EI}(3l_e - z_1)$$

For the tests with only one displacement transducer at pile top (TU Delft and CUED), the rotation at soil surface was estimated,

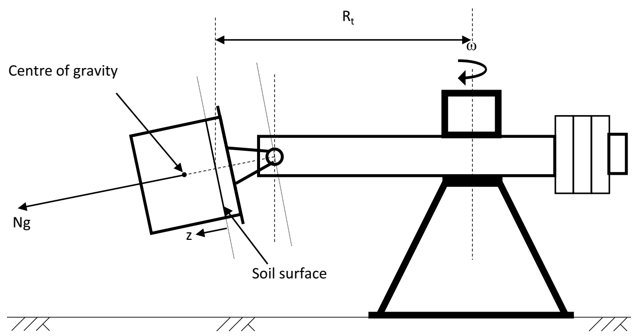


**Figure 1.** Schematic illustration of a beam centrifuge

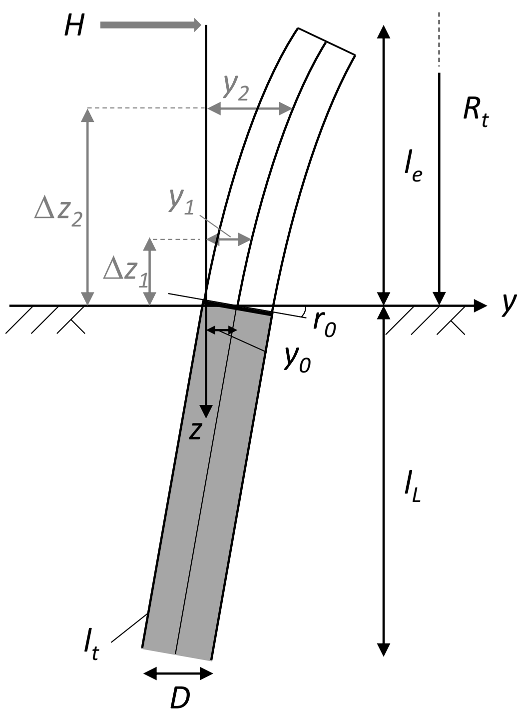


**Figure 2.** Displaced monopile, showing position of two displacement transducers and centre displacement profile (schematic)

assuming a rigid pile with a given rotation point slightly above the middle of pile penetration depth. This leads to the following equation:

6. $$y_0 = y_{top}\frac{0.43l_L}{l_e + 0.43l_L}$$

This simplified approach was calibrated to match the tests with two displacement measurements. This is a simplification, and the basis for this assumption is limited to observations from other tests in this study.

The test programme was designed to investigate modelling effects that need to be considered when performing monopile testing in a centrifuge, and as such it comprises three parts. The sand preparation was performed using dry pluviation at all centrifuge facilities to achieve a similar structure of the sand, characterised by its void ratio or relative density. In the first part, modelling of model studies was performed in two centrifuge facilities independently (local benchmark testing). Here, the same prototype response is modelled using differently sized model monopiles at corresponding centrifuge accelerations. This demonstrates the validity of the linear normalisation that is commonly used. In the second part, benchmark tests are performed across different centrifuges (global benchmark testing), again modelling the same prototype response. This allows investigation of the effects of sand sample preparation, loading, and other boundary conditions across the centrifuge facilities. This benchmark is performed at two different stress levels. Finally, the effect of pile installation and pile penetration depth is explored. Overview of the complete testing programme is provided in Table 1, which shows the values achieved during the testing.

For the first two parts of the test schedule, a stress condition similar to a prototype pile with a diameter of $D \sim 2$ m and 5 m, a load eccentricity of $l_e/D \sim 4$, and penetration $l_L/D \sim 5$ embedded into a dry homogeneous sand with a relative density of 80% was the aim.

To investigate the effect of pile penetration depth four tests were performed for stress conditions similar to a prototype pile of $D \sim 2$ m all with stress similarity in a depth of 2/3 of the pile penetration depth, a load eccentricity of $l_e/D \sim 5.3$ and normalised penetration depth $l_L/D \sim 4.0$–5.3 to 6.6–7.9 in dry homogeneous sand, dry pluvated to a relative density of $D_r$ = 75%. All sand samples had the same height, and the pile tip was sufficiently away from the container bottom to avoid any boundary effects.

Finally, the effect of installation method on the lateral response was investigated in stress conditions similar to a prototype pile with a diameter of $D \sim 5$ m, a load eccentricity of $l_e/D \sim 4$, and penetration $l_L/D \sim 3.2$ in dry homogeneous sand with a relative density $D_r$ = 33%. A relatively loose sample was used here due to the limitation of the maximum achievable driving force during in-flight installation.

The test setup varies from centrifuge to centrifuge. Table 2 presents the main boundary conditions and measurement setups used across the centrifuges. The column 'No of disp. Trans.' Refers to the number of displacement transducers used to measure pile displacement above the sand surface. Two different types of containers were used, cylindrical and square. Table 2 gives the dimensions and finally the description of the soil–pile interface. Sand was not observed to bond to any of the piles, and all model piles are regarded as having a smooth interface.

The experimental procedure in all facilities comprised of an installation phase, a lateral loading phase, and in some of the tests, a cone penetration phase. The installation was carried out under 1 g conditions with the exception of the study investigating the effect of installation.

## 3. Test results

### 3.1 Laboratory testing

The sands used at the different centrifuge facilities were first tested in the laboratory at NGI. All are poorly graded fine silica

**Table 1.** Test programme

| Test | $R_t$: m | $\omega$: 1/s | $D$: mm | $t$: mm | $l_L$: mm | $l_e$: mm | $z_1$: mm | $z_2$: mm | $E_{pile}$: Gpa | $\gamma$: kN/m$^3$ | $D_r$ |
|---|---|---|---|---|---|---|---|---|---|---|---|
| CEIGR_1 | 1.609 | 14.87 | 50 | 3.2 | 250 | 200.1 | 48.8 | 148.8 | 69 | 16.46 | 0.79 |
| CEIGR _2 | 1.610 | 14.87 | 50 | 3.2 | 250 | 200.9 | 49.6 | 149.6 | 69 | 16.46 | 0.79 |
| CEIGR _3 | 1.609 | 23.46 | 50 | 3.2 | 250 | 199.6 | 48.3 | 148.3 | 69 | 16.50 | 0.81 |
| CUED_1 | 3.725 | 11.37 | 38 | 1.71 | 200 | 200 | — | 200 | 70 | 15.08 | 0.75 |
| CUED_2 | 3.725 | 11.36 | 38 | 1.71 | 250 | 200 | — | 200 | 70 | 15.08 | 0.75 |
| CUED_3 | 3.725 | 11.33 | 38 | 1.71 | 300 | 200 | — | 200 | 70 | 15.08 | 0.75 |
| CUED_4 | 3.725 | 11.39 | 38 | 1.71 | 150 | 200 | — | 200 | 70 | 15.08 | 0.75 |
| COFS_1 | 4.655 | 9.02 | 52.2 (50#) | 2.1 (1) | 250 | 197 | 22 | 126 | 200 | 16.81 | 0.80 |
| COFS_2 | 4.655 | 14.27 | 52.2 (50#) | 2.1 (1) | 250 | 197 | 22 | 126 | 200 | 16.81 | 0.80 |
| COFS_3 | 4.655 | 14.39 | 52.2 (50#) | 2.1 (1) | 159.2 | 197 | 22 | 126 | 200 | 14.99 | 0.20 (0.33*) |
| COFS_4 | 4.655 | 14.39 | 52.2 (50#) | 2.1 (1) | 159.2 | 197 | 22 | 126 | 200 | 14.99 | 0.20 (0.33*) |
| COFS_5 | 4.655 | 14.39 | 52.2 (50#) | 2.1 (1) | 159.2 | 197 | 22 | 126 | 200 | 14.99 | 0.20 (0.33*) |
| COPPE_1 | 0.570 | 39.48 | 19.2 | 1.3 | 96 | 77 | 7 | 62.3 | 70 | 15.7 | 0.73 |
| COPPE_2 | 0.570 | 39.48 | 19.2 | 1.3 | 96 | 77 | 7 | 62.3 | 70 | 15.7 | 0.73 |
| COPPE_3 | 0.570 | 39.48 | 19.2 | 1.3 | 96 | 77 | 7 | 62.3 | 70 | 15.9 | 0.79 |
| DTU_1 | 2.290 | 14.21 | 40 | 2 | 200 | 160 | 38.0 | 58.0 | 210 | 16.33 | 0.77 |
| DTU_2 | 2.290 | 14.22 | 40 | 2 | 200 | 160 | 38.0 | 58.0 | 210 | 16.38 | 0.78 |
| UGE_1 | 4.778 | 6.20 | 100 | 5 | 500 | 400 | 38 | 400 | 74 | 16.15 | 0.73 |
| UGE_2 | 4.778 | 8.91 | 50 | 2.5 | 250 | 200 | 35 | 200 | 74 | 16.15 | 0.73 |
| UGE_3 | 4.778 | 9.99 | 40 | 2 | 200 | 160 | 38 | 160 | 74 | 16.15 | 0.73 |
| UGE_4 | 4.778 | 13.56 | 22 | 11 | 110 | 88 | 38 | 88 | 74 | 16.15 | 0.73 |
| TU Delft_1 | 1.035 | 31.42 | 18.2 | 1.2 | 90 | 72 | — | 72 | 74 | 15.57 | 0.80 |
| TU Delt_2 | 1.035 | 31.42 | 18.2 | 1.2 | 90 | 72 | — | 72 | 74 | 15.57 | 0.80 |
| KAIST_1 | 4.44 | 7.32 | 80 | 1.5 | 400 | 320 | 70 | 445 | 190 | 15.38 | 0.77 |
| KAIST_2 | 4.44 | 11.58 | 80 | 1.5 | 400 | 320 | 70 | 450 | 190 | 15.40 | 0.77 |
| KAIST_3 | 4.44 | 9.82 | 80 | 1.5 | 400 | 320 | 70 | 450 | 190 | 15.35 | 0.76 |
| KAIST_4 | 4.44 | 8.79 | 100 | 2.6 | 500 | 400 | 100 | 500 | 190 | 15.34 | 0.77 |
| KAIST_5 | 4.44 | 11.34 | 60 | 1.6 | 300 | 240 | 79 | 313 | 190 | 15.35 | 0.75 |
| UoN_1 | 1.53 | 13.76 | 60 | 3 | 300 | 240 | 60 | 240 | 69 | 16.9 | 0.90 |
| UoN_2 | 1.53 | 21.77 | 60 | 3 | 300 | 240 | 60 | 240 | 69 | 17.0 | 0.93 |

#Pile has an epoxy coating, the values in parenthesis () are the steel dimensions. Values given in the table are steel + epoxy
*Adjusted based on CPT tests performed at 100 g

**Table 2.** Info on experimental setups used at the different centrifuge facilities

| Facility | Vertical fixity | No of disp. Trans. | Container*: mm | Pile surface material |
|---|---|---|---|---|
| CEIGR | Free | 2 | 500 | Aluminium |
| COFS | Free | 2 | 1000 × 500 | Epoxy on steel |
| COPPE | Free | 2 | 220 | Aluminium |
| CUED | Free | 1 | 600 | Aluminium |
| DTU | Fixed | 2 | 500 | Steel |
| UGE | Free | 3 | 1000 × 500 | Aluminium |
| KAIST | Free | 4 | 1000 × 500 | Steel |
| Tu Delft | Free | 1 and 2 | 400 × 200 | Aluminium |
| UoN | Free | 2 | 490 | Aluminium |

*The single value refers to the diameter of a cylindrical container, $L \times W$ refer to side length and width of a square container

sands. A photo of the sands are given in Figure 3, it is seen that all sands looks very similar (grain-size, shape, and colour) with the sand from CEIGR and UoN slightly more reddish. The grain size distributions are shown together with the average grain size diameter in Figure 4. The maximum and minimum dry unit weight of sand is known to depend on the testing methodology, and it is therefore difficult to define a unique value (Blaker *et al*., 2015). However, relative density is commonly used to describe the state of sand, and this is the reason for using it here also. The maximum and minimum dry unit weight were determined based on the methodology used by the NGI laboratory as described in Blaker *et al*., 2015. Because all sands were tested in the same laboratory, the methodology is the same between the tests, which enhances the comparison of the achieved relative density. Table 3 describes the sands.

All sands were also tested under drained isotropic compression in the NGI laboratory. Berre (1981) described the triaxial setup at NGI, with rough endplates, sample diameter of 70 mm, and

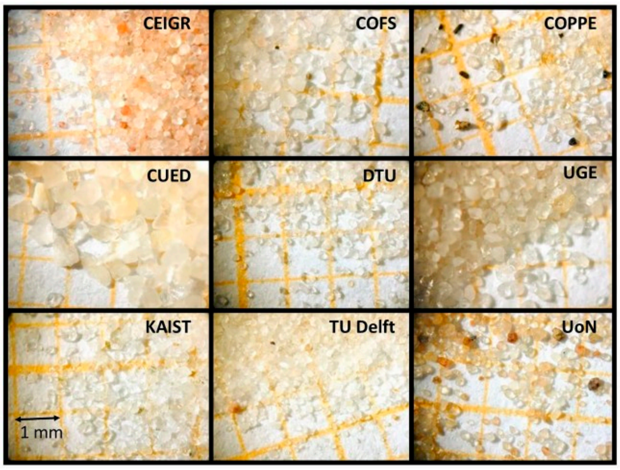


**Figure 3.** Close-up photo of the sand grains used in the centrifuge tests

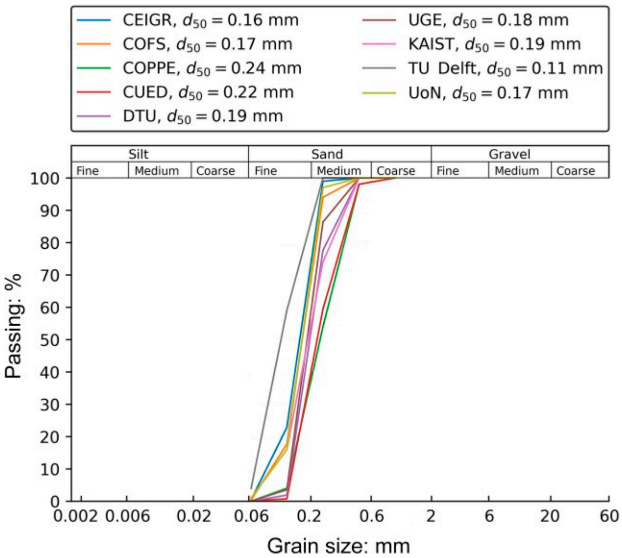


**Figure 4.** Grain size distribution of the different sands

**Table 3.** Dry density of the tested sands

| | Minimum dry density: g/cm$^3$ | Maximum dry density: g/cm$^3$ | Solid density: g/cm$^3$ |
|---|---|---|---|
| CEIGR | 1.48 | 1.74 | 2.64 |
| COFS | 1.48 | 1.79 | 2.66 |
| COPPE | 1.40 | 1.69 | 2.64 |
| CUED | 1.32 | 1.63 | 2.63 |
| DTU | 1.44 | 1.75 | 2.64 |
| UGE | 1.43 | 1.74 | 2.65 |
| KAIST | 1.31 | 1.66 | 2.64 |
| TU Delft | 1.32 | 1.67 | 2.63 |
| UoN | 1.75 | 1.49 | 2.64 |

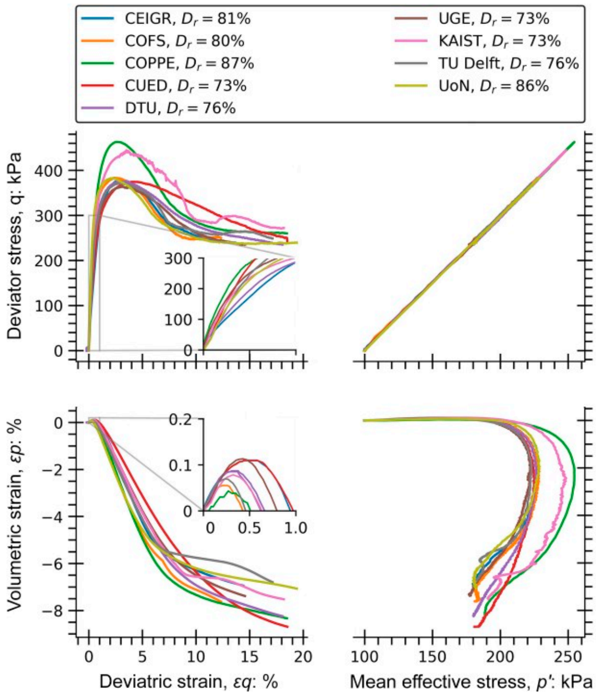


**Figure 5.** Test results of triaxial drained isotropic compression. Negative volumetric strains indicate increase in volume

diameter to length ratio of 2. The sands were reconstituted by dry pluviation (to simulate sand sample preparation for the centrifuge tests) and were isotopically consolidated to a mean effective stress of 100 kPa. Before shearing, the shear wave velocity ($\sim G_0$) was measured using bender elements. The $G_0$ measurements showed some scatter between 80 and 150 MPa. The shearing was performed by increasing the vertical load and keeping the radial stress constant. The results of the triaxial tests are shown in Figure 5.

All sands provide similar results, even though the relative density achieved varies. The maximum mobilised angle of friction is found to be between 40° and 41° for most of the sands except the one from KAIST and COPPE, which was found to be 44°. The dry pluviation technique makes it difficult to control the achieved density in the small triaxial samples, and the relative density achieved for the test of the COPPE sand was high which may be one explanation for the stronger resistance at peak. No tendency between peak strength and relative density was seen for the test with the sand from KAIST.

### 3.2 Cone penetration tests testing

CPTs were carried out in three of the facilities (COFS, DTU, and UGE) before the respective lateral load tests. At COFS also tests after the lateral load test were also performed. The mini penetrometers used in these tests have diameters of $D_{CPT}$ = 7–11 – 12 mm (COFS–DTU–UGE). Penetrations took place at acceleration levels reported in Table 1. All test results show a fairly linear increase with depth (Figure 6(a)) indicating that the soil samples are homogeneous. The tip resistance increases with penetration depth and with stress level, hence all the CPTs performed plot consistently with the expected behaviour. All tests at UGE were performed in the same sand sample, and the different responses are therefore likely to be linked to the effect of the stress level. The results from COFS demonstrate the effect of the relative density, with a smaller cone resistance for a lower relative density. Several CPT tests were carried out at DTU (1 for each test) and COFS (6 in dense and 6 in loose samples) to confirm consistency in the results. The satisfactory repeatability of tests confirms the soil mechanical behaviour; hence, the sample preparation method can be considered to produce samples that are similar for the tests where CPTs were performed. The sand preparation was done as dry pluviation at all centrifuge facilities, and the CPT tests indicate that this technique provides sand samples with satisfactory repeatability for sample where CPTs were also not performed. Figure 6(b) shows normalised test results, here calibrated to provide an estimate of relative density. The normalisation is based on Schneider and Lehane (2006) but here adjusted to correspond with the observations from the average relative density based on final weight and volume of samples. The tests from UGE plot on top of each other except for the first test (UGE_1). The difference in response may be due to the fact that the sample is denser in the position where the test was carried out, but can also be related to stress level effects that do not normalise linearly. This test was performed at a relatively low stress level, which leads to a higher degree of dilatancy and thereby also soil strength. It is, though, impossible to validate these hypotheses, and it is the author's attempt to explain the observations seen in the centrifuge tests. The results from the rest of the UGE tests, DTU, and COFS_2 plot closely. The results indicate that the tests at UGE are carried out at a lower relative density than tests at DTU and COFS, which is confirmed by the average relative density calculated based on the weight and volume of the sample. Table 1 shows the achieved average relative density for each test. The application of well – known (Baldi *et al*. (1981) and Jamiolkowski *et al*. (2001) expressions of relative density estimation from cone penetration results in the present centrifuge tests has not provided results that correspond to the estimates based on weight and volume. The simple normalisation as proposed in Figure 6 seems to give a better prediction of the relative density for these tests. This could be associated with the different stress field and the associated penetration deformations in the calibration chamber compared with the ones in the centrifuge, and the size of the cones. The achieved average relative density (found by measuring the weight and volume of the sample) of the loose sand sample at COFS was found to be smaller than the estimate from the CPT normalisation. This difference is most likely linked to the fact that this loose sand sample was densifying during the increase of acceleration in the tests, and the CPT estimate of relative density is therefore here regarded as a better measure for these tests. The denser sand samples were not subjected to the same volume change during centrifuge acceleration, which is confirmed by the CPT test results.

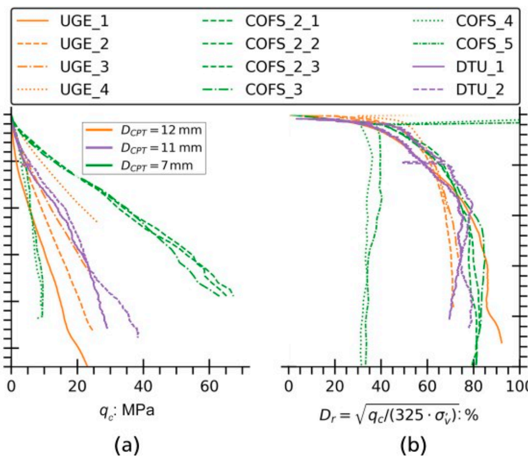


**Figure 6.** CPT results and normalisation

## 3.3 Local benchmark testing – modelling of models testing

The modelling of model methodology was used here to highlight whether any scale effects related to the non-scaling of sand grains are present. This method (e.g. Ovesen, 1979 for shallow foundations, and Schofield (1980)) is rarely used for monopiles in the physical modelling practice. The tests aim to demonstrate that foundations with different sizes can be used to model the same prototype behaviour if effective stresses are scaled correctly.

Four modelling of model's tests were carried out on model piles with different diameters at UGE ($D/d_{50}$ = 122–222 – 278–556) and three tests were carried out at KAIST ($D/d_{50}$ = 316–421 – 526). The tests were designed so that the soil stresses along the pile in tests were identical at each of the centrifuge facilities, such that tests scale to the same prototype pile. The effective stresses correspond to a prototype pile with a diameter of 2 m for the UGE tests and 3.6 m for the KAIST tests. The results of this local benchmarking are shown in Figure 7. The normalised results from the UGE tests are shown in Figure 7(a), and the corresponding tests from KAIST are shown in Figure 7(b).

For laterally loaded slender piles, there are no significant scale effects detected in modelling of model tests for $D/d_{50}$ > 60 as reported in Garnier *et al*., 2007. In the case of close-ended monopiles, Klinkvort *et al*. (2013b) did not see any effect for pile

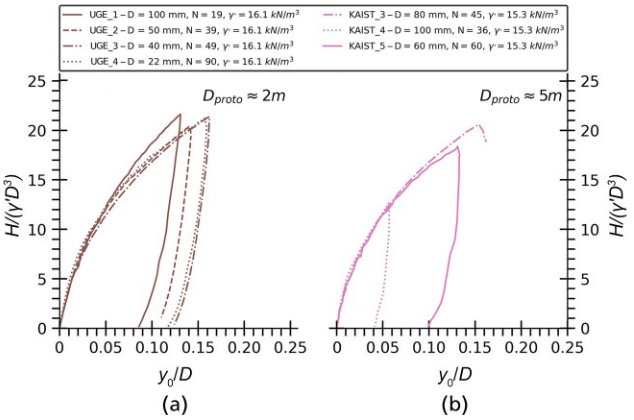


**Figure 7.** Test results of local benchmark tests, of prototype pile installed in dry sand with stress distribution similar to a pile with a diameter of (a) $D_{\text{proto}} \sim 2$ m, UGE: $D/d_{50} = 122$–$556$ and (b) $D_{\text{proto}} \sim 5$ m, KAIST: $D/d_{50} = 316$–$526$

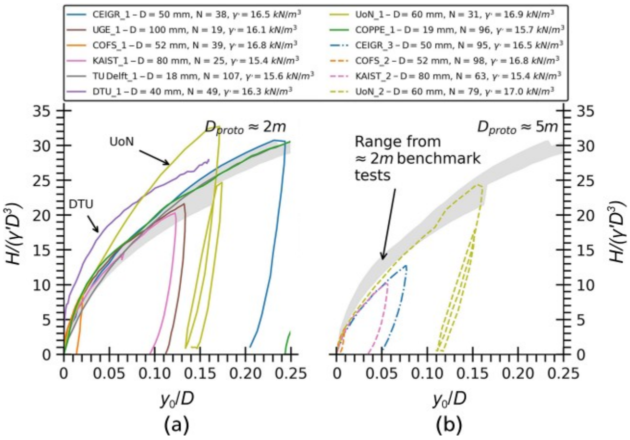


**Figure 8.** Test results of global benchmark tests, of prototype pile installed in dry sand with stress distribution similar to a pile with a diameter of (a) $D_{\text{proto}} \sim 2$ m and (b) $D_{\text{proto}} \sim 5$ m. $D/d_{50} = 313$ (CEIGR) – 306 (COFS) – 79 (COPPE) – 211 (DTU) – 556 (UGE) – 421 (KAIST) – 163 (TU Delft) – 353 (UoN)

diameters larger than $D/d_{50} > 100$. In the present modelling of model's study, the smallest pile has a diameter to average grain-size ration of $D/d_{50} > 122$, and the test results here also show no grain-size effects.

There is a small inconsistency in the UGE tests; the pile with a diameter of $D = 100$ mm shows a slightly stiffer normalised response. This pile was installed at $3.5D$ from the container wall in the direction perpendicular to loading and more than $8D$ in the loading direction. Moreover, the distance from the pile base to the bottom of the strongbox was larger than $2D$. The reason for the stiff response does therefore not seem to be related to boundary effects. Even with this inconsistency, the modelling of model's tests shows consistent results for each of the two benchmark cases, confirming the normalisation technique and thereby no grain-size effects.

### 3.4 Global benchmark testing

With the modelling of model's exercise confirming the normalisation technique shown in Equation 2 and the modelling technique, two series of tests, with different stress levels, across the different centrifuges were carried out. The results are shown in Figure 8 for stress levels corresponding to a $D \sim 2$ m monopile (a) and for stress levels corresponding to a $D \sim 5$ m monopile (b).

Figure 8 shows the normalised lateral pile head response for 8 different tests performed at a stress level similar to a 2 m in diameter pile and for four different tests performed at a stress level similar to a 5 m in diameter pile. A good match between the normalised results in the tests from CEIGR ($D/d_{50} = 313$), UGE ($D/d_{50} = 556$), COFS ($D/d_{50} = 306$), TU Delft ($D/d_{50} = 163$), KAIST ($D/d_{50} = 421$), and COPPE ($D/d_{50} = 79$) is seen on Figure 8(a), and also a good match is seen between the tests from CEIGR, COFS, KAIST, and UoN on Figure 8(b).

The response in Figure 8(a) for the UoN test shows a good agreement in the initial part of the load displacement curve ($y_0 < 0.025$D) but starts to deviate at higher displacements. The reason for this difference may be related to the relative density that was $D_r = 90\%$ for this test and therefore higher than the rest of the tests that had relative densities between $D_r = 73\%$–$80\%$. The test from UoN on Figure 8(b) for the higher stress levels shows a better agreement with the other tests. This indicates that the difference seen is not related to the UoN test setup. The response from the tests at DTU (Figure 8(a)), on the other hand, shows a significantly stiffer response. This is most likely related to the way the load is applied to the pile head at DTU. At DTU, the load is applied in a way that allows rotation, but not vertical displacements. This is different from the other setups, where the lateral load is applied in a way that will enable both free pile head rotation and vertical pile head displacements. The fixed vertical constraint at DTU enables the measurement of vertical forces, and large downward axial loads ($V_{\text{max}} < 6000$ N) were observed during the tests, resulting in distinct load conditions compared with the other tests. Even with the disparities seen in the two tests, the general observations are clear. It is possible to model the same prototype monopile response using different geometries and centrifuge setups if care is taken to ensure the soil state and boundary conditions.

### 3.5 Stress level effect testing

Figure 8 also shows the effect of stress level; here monopiles with identical non-dimensional geometry were tested at different acceleration levels. The range of results from local benchmark ($D_{\text{proto}} \sim 2$ m) tests from UGE, together with the six reliable tests from the global benchmark ($D_{\text{proto}} \sim 2$ m), are shown with a grey area on both panels (a) and (b).

The tests correspond to stress conditions similar to prototype monopiles with diameters for $D_{\text{proto}} \sim 2$–5 m. The grey area on panel (b) allows a comparison of the normalised response for the two stress levels. The tests performed at the higher stress level ($D_{\text{proto}} \sim 5$ m) show a softer response. This is because the sand at lower stress levels experiences higher dilatancy and mobilised strength. The low stress effect is seen as an increase in the normalised response, like that reported in Klinkvort and Hededal (2014). This illustrates that the normalisation is only valid for a given stress level and that it is therefore essential to perform tests at stress levels corresponding to the target prototype behaviour. Testing at too low stress levels will lead to an overestimation of stiffness and strength using the normalisation presented here. On the other hand, the effect of stress is decreasing with increasing stress, and that is also why we only see a small difference between the results here. This was also seen in the study by Klinkvort and Hededal (2014) for monopiles and for triaxial testing by Bolton *et al*. (1999).

### 3.6 Effect of pile penetration depth

Figure 9 shows the effect of pile penetration depth, with all other geometries kept constant (diameter, $D$ = 38 mm and load eccentricity, $l_e = 5.25D$). Here, the normalised horizontal load has been scaled to be able to compare with the other tests performed with a different load eccentricity ($l_e = 4D$). The horizontal load has been scaled down with the ratio between the load eccentricities of 4/5.25. This attempt to correct the different applied moments thereby allows an approximate comparison with the rest of the tests. Again, the range of results from the benchmark ($D_{\text{proto}} \sim 2$ m) tests is shown with a grey area.

The results from the CUED tests fall into the range seen from the benchmark tests. The test with pile penetration of $l_L$ = 5.25D (CUED_1) is the one with a monopile geometry that is closest to the benchmark tests and it shows a slightly softer response. The tests with longer penetration (CUED_2 and CUED_3) show a stiffer response, and the test with less penetration shows a softer response (CUED_4). The response of the pile with the lowest penetration depth, CUED_4, shows a remarkably softer response. This was also observed in previous centrifuge test results in dense sand (Zania *et al*., 2015) and in a parallel test series on looser sand. Beyond this penetration depth, however, the results show that differences in pile penetration depth affect the capacity but not the initial stiffness. This is linked to the initial response being governed by pile stiffness itself and the upper soil resistance. At higher loads, the soil along the full pile is mobilised, and the effect of pile length is then evident.

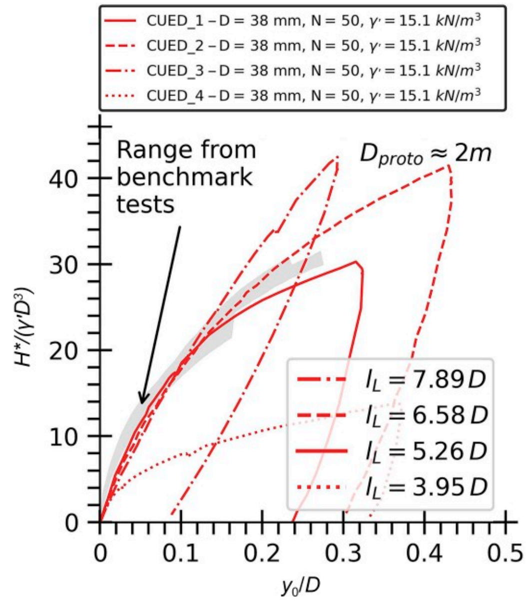


**Figure 9.** Test results of piles tested with different penetration depths and constant load eccentricity, $l_e = 5.25\,D$. $H^*$ indicates that the horizontal load has been scaled with a factor of 4/5.25 for the CUED tests

### 3.7 Effects of pile installation

The effect of the pile installation method on the lateral response was investigated using jacking and impact driving at 1 g and $N_g$. Two tests were carried out with in-flight installation and lateral loading without stopping the centrifuge to retain the installation-induced stress state (post-pile driving). The setup allows for the pile installation to commence from the soil surface, with the pile suspended until the installation is initiated at the target centrifuge acceleration. The jacked installation was performed by applying a constant penetration rate of 0.5 mm/s through the actuator. Impact driving was modelled using the miniature pile driving hammer developed by Bruno and Randolph (1999). A ram weight of 50 g and drop height of 17 mm were used together with a driving frequency of 5 Hz, all at model scale. The tests and setup are also described in Fan *et al*. (2019). After installation, the connection between the pile head and the pile driver was released in-flight to create a free-end condition. Lateral loading was then applied following the installation until the monopile sand surface displacement exceeded 0.1$D$. The tests were conducted (including a test featuring jacked installation at 1 g for comparison) in a medium dense sand sample ($D_r$ = 35%), to ensure the loading rig was not overloaded and a sufficient penetration depth was achieved (3.2$D$).

The results of the lateral response of monopiles installed by jacking at 1 g, jacking at $N_g$, and impact driving at $N_g$ are shown in Figure 10. Here, it is shown that a monopile jacked in-flight

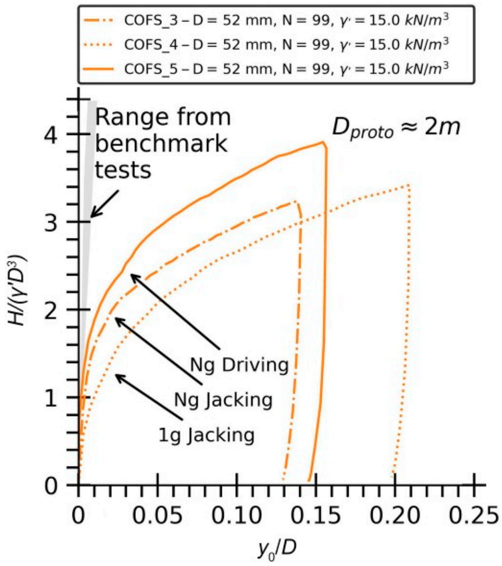


**Figure 10.** Results of lateral loaded pile with different installation methods

(COFS_3) yields larger initial stiffness than a pile jacked at 1 g (COFS_4) due to the stress level effect. This is in agreement with the observations made by Dyson and Randolph (2001) and Klinkvort (2012). In contrast, a monopile installed using impact driving (COFS_5) shows larger initial stiffness and higher ultimate capacity than the jacked pile (COFS_3). The stress level during installation was identical in these two tests. Therefore, the increased stiffness and ultimate capacity are underpinned by the changes in soil states caused by impact driving.

## 4. Discussion and recommendations

The experimental results have shown that with a careful test design, centrifuge modelling enables modelling of similar prototype responses using different sands, piles, and setups. This was demonstrated using relatively simple monotonic tests, but it is natural to assume these findings are also applicable to more advanced cyclic tests.

Monopile supporting offshore wind turbines installed in layered saturated soil deposits are also subjected to repeated multidirectional loading. It is therefore also clear that more advanced testing is necessary to develop new design models. We aim to highlight some of the key learnings and discussions that we have had during this project, and we believe that these insights will be essential for designing new centrifuge test programs.

New tests should be conducted in conjunction with numerical finite element analysis to enhance test interpretation. The soil sample used in the testing should be characterised as good as possible. This is the only way a reliable interpretation of the modelling can be achieved. A combination of element testing of the sand and model classification using CPT is recommended. This was partially achieved in this study through sand classification and triaxial testing of all sand, as well as CPT in some of the test containers. CPT testing in the test container is the best way to validate the homogeneity of the sample. The sand element test programme depends on the centrifuge test programme; however, it is recommended to include an accompanying cyclic triaxial test programme when performing cyclic-loaded centrifuge tests. It is also recommended to mount vertical and horizontal stress sensors in the container or bender elements to obtain a more accurate estimate of the soil stiffness and stresses. This, together with laboratory testing of the sands and CPT, enables the interpretation of the state (density and stress) of the sand sample and enhances the comparison with, for example, numerical finite element models.

The tests presented in this paper are monotonic tests performed in dry sand, which, of course, differs from prototype monopiles installed offshore in saturated sand. The sand response is a function of the effective stress, and because the monotonic tests are fully drained, the results can also be interpreted as tests in saturated sand but with a larger geometry (diameter and pile length). For example, the benchmark tests performed with stresses that correspond to a monopile with a diameter of $D$ = 2–5 m in dry sand will also correspond to a monopile in saturated sand with a diameter of $D$ = 3.2–8 m, see for example Klinkvort and Hededal (2013a). The stress conditions in these tests resemble, therefore, the stress conditions offshore.

The results of the study suggest that the installation process has a significant influence on the initial stiffness and ultimate capacity of monopiles under lateral loading. This is important to acknowledge and to be accounted for in centrifuge testing. One alternative is to perform tests without modelling the installation; here the pile should preferably be placed in the sand sample without disturbing the surrounding sand (which can be difficult to achieve with a fully homogeneous sand density around the pile and good initial contact with the pile). The effect of installation then needs to be addressed separately, for instance, through comparison with numerical modelling results. Another alternative is to include the effect of installation by using a pile driving hammer, as done here in the test COFS_5. This is possible but needs, as for real monopiles, specialised driving equipment. Further research on the effect of the installation process on the in-service response of monopiles, considering the role of the pore fluid response in saturated sand and the effect of cyclic loading, is needed.

Offshore monopiles are subjected to complex loading that needs to be understood for optimised design. The aim of this paper was to provide a validation of the modelling technique and to provide recommendations for centrifuge testing of laterally loaded monopiles, not only for monotonic loading but also looking towards more complex load scenarios. The effect of cyclic loading on a monopile in saturated sand from one or more directions is one of the most obvious effects that needs to be understood. The complexity of the loading raises some additional modelling requirements that need to be addressed to retain similarity, one of these being the ability to capture any potential pore pressure accumulation. These tests, therefore, need to be performed in a saturated sand where both viscosity and load frequency are scaled with the geometrical scaling factor. Here, reference should be made to the methodologies used for earthquake engineering, see, for example, Madabhushi (2014).

## 5. Conclusions

Offshore monopiles are subjected to complex loading that needs to be understood for optimised design. This paper has illustrated that centrifuge modelling provides an effective tool to gather physical evidence of the response of monopiles. Through a series of multi-facility benchmark tests, the modelling approach has been validated, including both local and global benchmark exercises at two stress levels. The validation was conducted using various centrifuge sizes, different container geometries, different sands, and different load setups, thereby highlighting the ability to investigate effects seen at a larger scale using small model-scale test setups. This is only possible if the non-dimensional monopile geometry and the sand state are similar between the different scales. Furthermore, the test results demonstrate that altering the non-dimensional monopile geometry and installation methodology has a significant impact on the results. These are all crucial observations that need to be addressed when performing centrifuge modelling.

## Acknowledgement

The laboratory testing at NGI was financially supported by the base funding from the Research Council of Norway (NRF). This work forms part of the activities of the Centre for Offshore Foundation Systems (COFS), which at the time of testing was supported as a Centre of Excellence by the Lloyd's Register Foundation. The Centre for Energy and Infrastructure Ground Research (CEIGR) is supported by the UK Engineering and Physical Sciences Research Council (EPSRC). The authors gratefully appreciate this support.

### REFERENCES

Baldi G, Bellotti R, Ghionna V, Jamiolkowshi M and Pasqualini E (1981) Cone resistance of a dry medium sand, In: *Proceedings of 10th International Conference on Soil Mechanics and Foundation Engineering,* vol. 2, pp. 427–432.

Bayton S and Black J (2016) The effect of soil density on offshore wind turbine monopile foundation performance. *Eurofuge* **1**: 245–251.

Berre T (1982) Triaxial testing at NGI. *Geotechnical Testing Journal* **5(1/2)**: 3–17.

Bienen B, Fan S, Schröder M and Randolph MF (2021) Effect of the installation process on monopile lateral response. *Proceedings of the Institution of Civil Engineers – Geotechnical Engineering* **174(5)**: 530–548.

Blaker Ø, Lunne T, Vestgården T *et al.* (2015) Method dependency for determining maximum and minimum dry unit weights of sands. In *Frontiers in Offshore Geotechnics*. CRC Press, vol. 162, pp. 1159–1166.

Bolton MD, Gui MW, Garnier *et al.* (1999) Centrifuge cone penetration test in sand. *Géotechnique* **49(4)**: 543–552.

Bruno D and Randolph MF (1999) Dynamic and static load testing of model piles driven into dense sand. *Journal of Geotechnical and Geoenvironmental Engineering* **125(11)**: 988–998.

Choo YW and Kim D (2016) Experimental development of the p-y relationship for large diameter offshore monopiles in sands: centrifuge tests. *Journal of Geotechnical and Geoenvironmental Engineering* **142(1)**.

Cuéllar P, Baeßler M and Rücker W (2009) Racheting convective cells of sand grains around offshore piles under cyclic lateral loads. *Granular Matter* **11(6)**: 379–390.

De Nicola A and Randolph M (1997) Centrifuge modelling of pipe piles in sand under axial loads. *Géotechnique* **49(3)**: 295–318.

Dyson GJ and Randolph MF (2001) Monotonic lateral loading of piles in calcareous sand. *Journal of Geotechnical and Geoenvironmental Engineering* **127(4)**: 346–352.

Fan S, Bienen B and Randolph MF (2019) Centrifuge study on effect of installation method on lateral response of monopiles in sand. *International Journal of Physical Modelling in Geotechnics* **21(1)**: 40–52, 10.1680/jphmg.19.00013.

Garnier J, Gaudin C, Springman S *et al.* (2007) Catalogue of scaling laws and similitude questions in geotechnical centrifuge modelling. *International Journal of Physical Modelling in Geotechnics* **7(3)**: 01–23.

Henke S and Grabe J (2008) Numerical investigation of soil plugging inside open-ended piles with respect to installation method. *Acta Geotechnica* 2008 **3(3)**: 215–223.

Henke B and Bienen S (2014) Investigation of the influence of the installation method on the soil plugging behaviour of a Tubular Pile, Physical Modelling in Geotechnics*. Proceedings of the 8th International Conference on Physical Modelling in Geotechnics 2014 (ICPMG2014)* pp. 681–687.

Jamiolkowski M, LoPresti DCF and Manassero M (2001) Evaluation of relative density and shear strength of sands from CPT and DMT. In *Soil Behavior and Soft Ground Construction*. ASCE, Reston, Virginia, pp. 201–238.

Kirkwood P (2015) *Cyclic lateral loading of monopile foundations in sand*, PhD Thesis, University of Cambridge.

Klinkvort RT (2012) *Centrifuge modelling of drained lateral pile soil response, Application for offshore wind turbine support structures*, PhD Thesis. DTU Orbit.

Klinkvort RT and Hededal O (2013a) Lateral response of monopile supporting an offshore wind turbine. *Proceedings of the Institution of Civil Engineers – Geotechnical Engineering* **166(2)**, pp. 147–158.

Klinkvort RT, Hededal O, Springman and SM (2013b) Scaling issues in centrifuge modelling of monopiles. *International Journal of Physical Modelling in Geotechnics* **13(2)**: 38–49.

Klinkvort RT and Hededal O (2014) Effect of load eccentricity and stress level on monopile support for offshore wind turbines. *Canadian Geotechnical Journal* **51(9)**: 966–974.

Klinkvort RT, Bayton T, Black S *et al.* (2018) A review of modelling effects in centrifuge monopile testing in sand. In *Physical Modelling in Geotechnics, 9th International Conference on Physical Modelling in Geotechnics.* Taylor & Francis Group, London, UK, pp. 719–724.

LeBlanc C, Houlsby GT, Byrne and BW (2010) Response of stiff piles in sand to long-term cyclic lateral loading. *Géotechnique* **60(2)**: 79–90.

Li Z, Haigh SK, Bolton and MD (2010) Centrifuge modelling of Mono-pile under cyclic lateral loads. In *Physical Modelling in Geotechnics*. Taylor & Francis Group, London, pp. 965–970.

Madabhushi G (2014) *Centrifuge Modelling for Civil Engineers*. CRC Press.

Mahutka KP, Grabe J and König F (2006) Numerical modelling of pile jacking, driving and vibratory driving, numerical modelling of construction processes in geotechnical engineering for urban environment. *Proceedings of the International Conference on Numerical Simulation of Construction Processes in Geotechnical Engineering for Urban Environment*, Bochum, Germany.

Ovesen NK (1979) The scaling law relationships, Design parameters in geotechnical engineering, *7th ECSMFE*, Brighton, **4**, 319–323.

Peralta P and Achmus M (2010) An experimental investigation of piles in sand subjected to lateral cyclic loads. In *Physical Modelling in Geotechnics*. Taylor & Francis Group, London, pp. 985–990.

Rudolph C, Bienen B and Grabe J (2014) Effect of variation of the loading direction on the displacement accumulation of large diameter piles under cyclic lateral loading in sand. *Canadian Geotechnical Journal* **51(10)**: 1196–1206.

Schneider J and A, Lehane BM (2006) Effects of width for square centrifuge displacement piles in sand, *Proc, 6th Int, Conf, Physical Modelling in Geotechnics*, vol. 2, Taylor & Francis, London, 867–873.

Schofield AN (1980) Cambridge geotechnical centrifuge operations. *Géotechnique* **30(3)**: 227–268.

Staubach P, Machaček J, Bienen B and Wichtmann T (2022) Long-term response of piles to cyclic lateral loading following vibratory and impact driving in water-saturated sand. *Journal of Geotechnical and Geoenvironmental Engineering* **148 (11)**.

Takahashi A, Omura N, Kobayashi T, Kamata Y and Inagaki S (2022) Centrifuge model tests on large-diameter monopiles in dense sand subjected to two-way lateral cyclic loading in short-term. *Soils and Foundations* **62(3)**: 101148.

Taylor RN (1994) *Geotechnical Centrifuge Technology*. CRC Press, Taylor & Francis.

Truong P and Lehane BM (2015) Experimental trends from lateral cyclic tests of piles in sand. In *Frontiers in Offshore Geotechnics III*, Norway.

Truong P, Lehane BM, Zania V, Klinkvort and RT (2019) Empirical approach based on centrifuge testing for cyclic deformations of laterally loaded piles in sand. *Géotechnique* **69(2)**: 133–145.

Wind Europe (2018) *Offshore Wind in Europe: Key Trends and Statistics 2017*, Brussels, Belgium.

Zania V, Hededal O, Klinkvort and RT (2015) Effect of relative pile's stiffness on the lateral pile response under loading of large eccentricity, *3rd International Symposium on Frontiers in Offshore Geotechnics*, Oslo, Norway **1**: 753–758.

## How can you contribute?

To discuss this paper, please email up to 500 words to the editor at support@emerald.com. Your contribution will be forwarded to the author(s) for a reply and, if considered appropriate by the editorial board, it will be published as discussion in a future issue of the journal.

*International Journal of Physical Modelling in Geotechnics* relies entirely on contributions from the civil engineering profession (and allied disciplines). Information about how to submit your paper online is available at www.emeraldgrouppublishing.com/journal/jphmg, where you will also find detailed author guidelines.